Journal of Optoelectronics and Advanced Materials Vol. 6, No. 4, December 2004, p. 1297 - 1303

EFFECT OF MECHANICAL STRAINS ON THE MAGNETIC PROPERTIES OF ELECTRICAL STEELS

V. E. Iordache*, E. Hug

Laboratoire Roberval, UMR UTC-CNRS, Université de Technologie de Compiègne, Département Génie Mécanique, BP 20529, 60205 Compiègne, France

The magnetic properties of steel laminations used as magnetic cores in electrical machines are very sensitive to mechanical strains resulting from manufacturing operations. This study presents an experimental in situ characterization of a non-oriented Fe-3%Si steel, a FeCo-2%V alloy and a high-purity polycrystalline nickel. The mechanical properties of study materials were determined under an monotonous uniaxial tensile test. Magnetic measurements were carried out under uniaxial tensile stresses approaching and exceeding the elastic limit σ_e, as well as in the corresponding unloaded states. The deformation stages are clearly identified by the magnetic parameters. A linear relationship was found between the evolution of the magnetic behaviour and of the kinematic hardening X, representative of internal stress state of plastically strained specimens.

(Received July 26, 2004; accepted November 29, 2004)

Keywords: Electrical steel, Tensile deformation, Magnetic measurements, Magneto-mechanical coupling, Internal stresses

1. Introduction

For an accurate design of electrical machines, the magnetic properties of steel laminations used as magnetic cores need to be precisely estimated. However, it is well-known that the material behaviour in the core is different - usually deteriorated - from the one measured under standard conditions. The main reason appears to be the presence of mechanical strains resulting from indispensable manufacturing operations like punching and core assemblage. An empirical factor to account for this difference is still used, because understanding and modelling the complex magnetomechanical interactions in core materials are still open problems [1, 4].

This study is in line with previous works of the same research team dedicated to a better understanding of the magnetization mechanisms of electrical steel in the presence of mechanical strains. Magnetic measurements were firstly performed on plastically strained unloaded specimens (after removal of the stress) of non-oriented Fe-3%Si and FeCo-2%V steel sheets, showing a strong degradation of the magnetic properties as an effect of plastic strain [1, 5-8]. This effect is more pronounced for low and medium values of magnetic field strength, corresponding to the reversible and irreversible motion of domain walls, which stands for the pinning effect of dislocations. Moreover, an attenuated magnetic degradation was observed in the direction perpendicular to the applied stress whatever the direction of the later inside the sheet plane. This directional effect, called "magnetoplastic anisotropy", seems to be directly linked to the internal stresses generated during strain-hardening [6]. As a first conclusion, these works showed that the magnetic degradation induced by the plastic deformation of the materials is the result of the joint effect of dislocations and internal stresses. The necessity of further studies directed to a better identification of these effects in the course of a simple mechanical test was also evidenced.

Thus, an appropriate experimental device allowing in situ magnetic measurements during an monotonous uniaxial tensile test was developed and results on a non-oriented Fe-3%Si steel were previously reported [9, 10]. This paper shows further interesting results on electrical steel, a high-

* Corresponding author: viordach@utc.fr

purity nickel and a FeCo-2%V ferromagnetic alloy obtained following this in situ methodology: Barkhausen noise and magnetic hysteresis measurements were carried out under stresses approaching and exceeding the elastic limit and in the all corresponding unloaded states. Firstly, the usual characteristics of the materials are given. The benchmark is then briefly described. The results of the magnetic measurements are presented and discussed in the last section, highlighting the effect of dislocations and internal stresses.

2. Experimental

2.1. Materials

Fer-silicium and FeCo-2%V laminations are of common use for the conception of electrical motors. The first study material was a "fully-process" non-oriented (NO) Fe-3%Si steel sheet of 0.35 mm thickness (French electrical steel FeV 330-35 HA). It is a body centred cubic (bcc) ferritic single-phase material, with a typical weak {111}<uvw> recrystallisation texture. Its grain structure is isotropic in volume and its average grain size is 50 µm. The FeCo-2%V alloy, received as 0.4 mm thick laminations, is an intermetallic ordered material which partly exhibits a B2 ordered structure [11]. Its average grain size is 30 µm and it presents a {111}<011> texture. Characterizations were also done on a high-purity polycrystalline nickel (99.98 %) received as 0.5 mm thick laminations. It presents a face centred cubic (fcc) crystallographic structure and an average grain size of 25 µm. Typical micrographs of the materials are shown in Fig. 1.

Mechanical behaviour was characterized under uniaxial tensile tests performed at room temperature at the constant strain rate $d\varepsilon/dt = 4 \times 10^{-4} s^{-1}$. The corresponding mechanical properties are shown in Fig. 1 and listed in Table 1. The stress-strain curves of Fe-3%Si and FeCo-2%V exhibit an initial yield drop, followed by a long Lüders strain plateau, typical for bcc metals. The homogeneous strain-hardening domain, which starts when the entire sample undergoes the Lüders band propagation, could be characterized by the evolution of the strain-hardening rate $\theta = d\sigma/d\varepsilon$. Two strain-hardening stages H.s.1 and H.s.2 are observed for Fe-3%Si (Fig. 1b), commonly related to the evolution of the dislocation feature. While the dislocation density increases proportionally to the square root of the plastic strain, clusters are progressively formed in the first stage, then walls of high dislocation density separated by regions of low dislocation density appear in the second stage [12]. FeCo-2%V shows a single linear homogeneous strain-hardening stage followed by a brittle fracture of the sample (Fig. 1d). The plastic deformation occurs by the movement of superlattice dislocations, which progressively organise themselves into tangles next to the grain boundaries [7]. Two strain-hardening stages are observed also for Ni (Fig. 1f): the first stage corresponds to single slip in {111} planes, while the second is associated with the formation of tangles and cells of dislocations.

Another important characteristic of the strain-hardening is the kinematic hardening X. According to Lemaitre-Chaboche model, X measures the translation of the centre of the elastic domain during strain-hardening and is representative of the internal stresses state of the material [13]. Following a methodology already employed for electrical laminations, which is based on the study of the morphology of the unloading stress-strain curves [6], the values of X for the studied materials were determined and represented on Fig. 1 too. It can be observed that a relatively high value is reached from the beginning of the strain-hardening of all the materials, followed by a slight increase until the maximal stress is reached.

2.2. Experimental device and methodology

In order to perform magnetic measurements during a mechanical test a single sheet tester device was adapted to an universal testing machine. Its fully description was given in [8], only the main features are presented here. Two ferrite yokes maintained in contact with the sample close the magnetic circuit. Two excitation coils (H-coils) are wound on the central limbs of the yokes and the measurement coil (B-coil) surrounds the sample – strip 20 mm width and 250 mm long. The magnetising current waveform is controlled by an operational amplifier.

Table 1. Average mechanical properties of studied materials under a monotonous uniaxial tensile test, $d\varepsilon/dt = 4 \times 10^{-4} s^{-1}$ (E, Young's modulus; σ_e^{max}, upper yield stress; σ_e^{min}, lower yield stress; L_p, Lüders strain length; σ_m, maximal stress; A, ultimate deformation).

	E (GPa)	σ_e^{max} (MPa)	σ_e^{min} (MPa)	L_p (%)	σ_m (MPa)	A (%)
Fe-3%Si	180 - 200	450 ± 20	430 ± 10	1.3 - 1.5	670 ± 10	20 - 30
FeCo-2%V	210 - 230	300 ± 10	280 ± 10	1.3 - 1.5	350 - 450	3 - 5
Ni	45 - 50	30 ± 5	-	-	390 ± 10	25 - 30

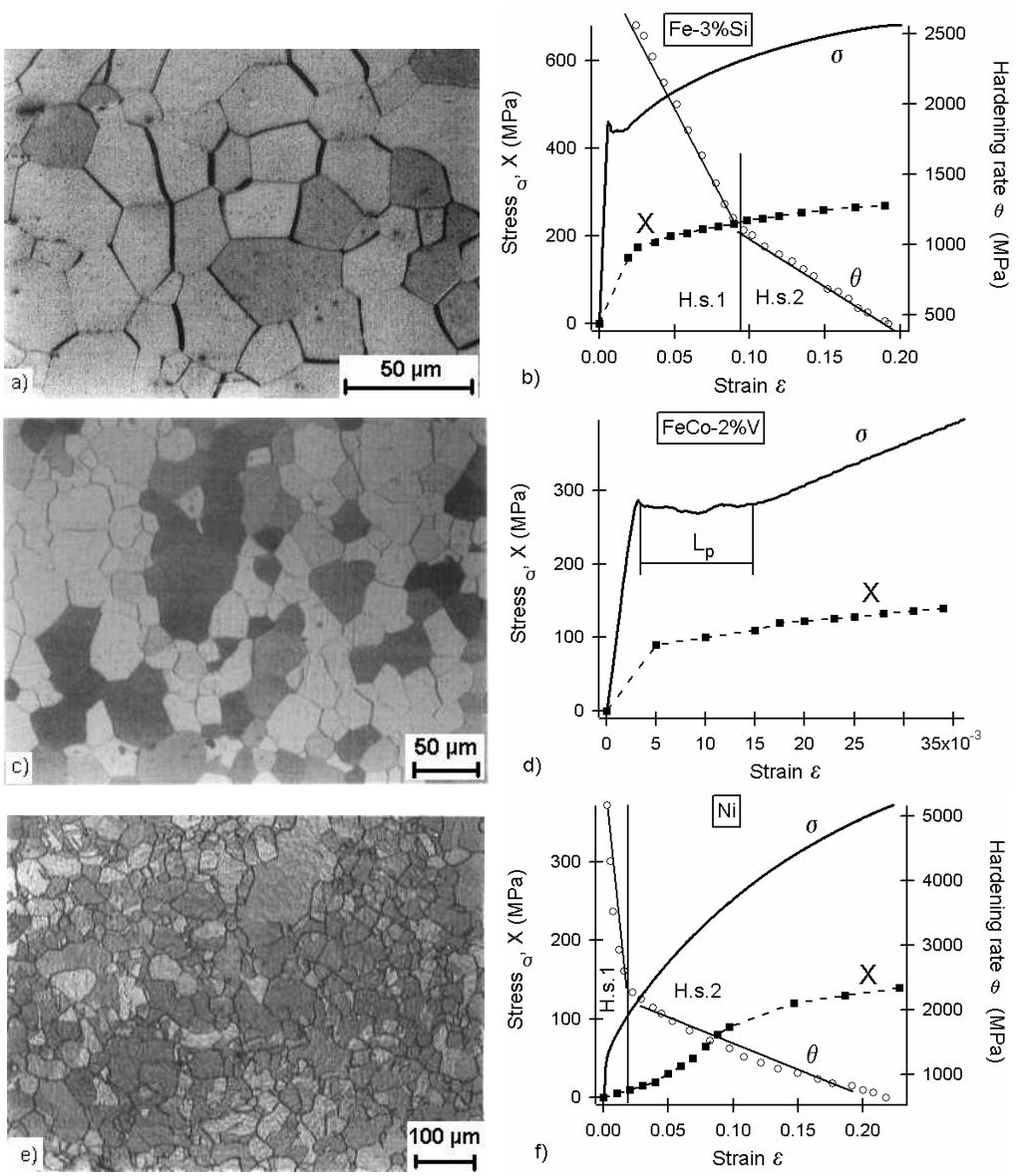

Fig. 1. Microstructure revealed by electrolytic etching, as well as typical true stress σ - true strain ε, kinematic hardening X and hardening rate $\theta = d\varepsilon/dt$ under a monotonous uniaxial tensile test ($d\varepsilon/dt = 4 \times 10^{-4} s^{-1}$, room temperature) for Fe-3%Si (a, b), FeCo-2%V (c, d) and Ni (e, f).

Magnetic hysteresis loops and normal magnetization curve are determined on the basis of the acquisition of the magnetising current and of the B-coil voltage. Moreover, Barkhausen noise is measured by band-pass filtering the B-coil voltage in the range of 0.5 to 250 kHz.

Magnetic measurements were carried out on the same specimen in the initial non-strained state, under stresses below and above the macroscopic elastic limit σ_e and in the corresponding unloaded states, after removal of the stress. For Fe-3%Si and FeCo-2%V, the first measurement point in the plastic strain domain was set at the beginning of the homogeneous strain-hardening. All the magnetic measurements were made under a 0.5 Hz sinusoidal magnetising current in the rolling direction RD of the laminations.

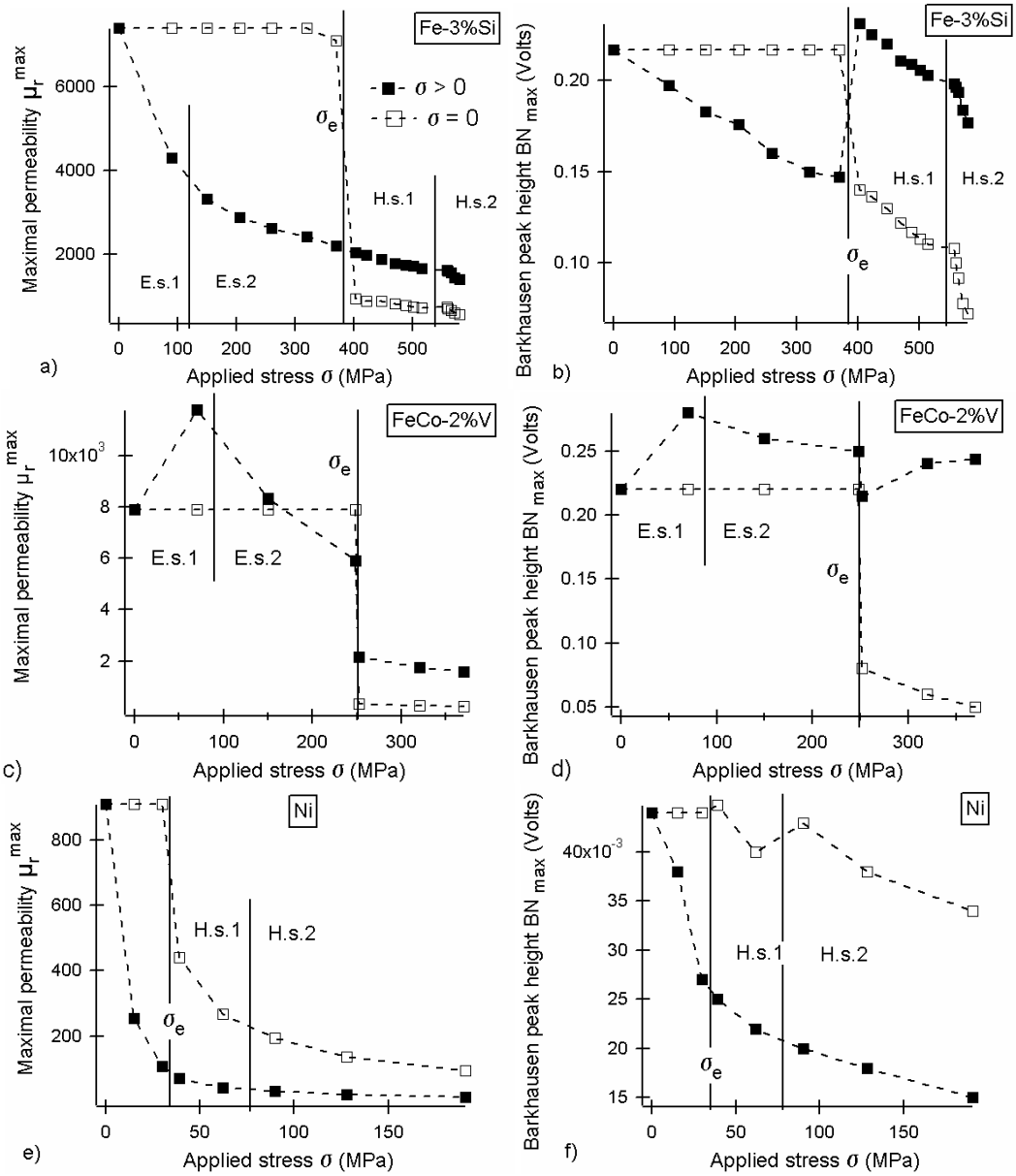

Fig. 2. Maximal relative permeability μ_r^{max} and Barkhausen noise peak height BN_{max} versus applied stress σ for under-stress states (full marks, $\sigma > 0$) and for the corresponding unloaded states (open marks, $\sigma = 0$) of the Fe-3%Si (a, b), FeCo-2%V (c, d) and Ni (e, f) specimens. Dashed lines are only for guidance. Delimitation lines mark the two elastic strain stages E.s. 1 and E.s. 2 for Fe-3%Si and FeCo-2%V, the macroscopic elastic limit σ_e and the two hardening stages H.s.1 and H.s.2 for Fe-3%Si and Ni.

3. Results

Fig. 2 shows several magnetic parameters measured for the loaded and the corresponding unloaded states of the Fe-3%Si, FeCo-2%V and Ni specimens. The relative permeability μ_r is calculated as the ratio between magnetic induction B and magnetic field strength H of the normal magnetization curve ($B/\mu_0 H$). Barkhausen noise is measured over a hysteresis loop from – 8 kA/m to + 8 kA/m, values corresponding to the magnetic saturation of the materials. Reproducibility tests show variations less than 3 % for all measured parameters.

In the elastic strain domain ($\sigma < \sigma_e$), for the under-stress measurements, the magnetic behaviour of Fe-3%Si and of Ni is deteriorated, as shown by the strong decrease of the maximal permeability (Fig. 2a, e). Barkhausen noise peak height BN_{max} is also diminished (Fig. 2b, f). An opposite behaviour is shown by FeCo-2%V alloy: the maximal permeability firstly increases, then decreases to a value lower than the initial one, while BN_{max} becomes higher than for the initial non-strained state (Fig. 2c, d). The magnetic parameters of Fe-3%Si and of FeCo-2%V show two elastic strain stages E.s.1 and E.s.2, delimitated by an evolution change for an applied stress close to 100 MPa. After removal of the stress, the magnetic properties are entirely recovered.

The demarcation between elastic strain and plastic strain domains is evidenced by the drop of μ_r^{max} and BN_{max} for FeCo-2%V and by the strong increase of BN_{max} for Fe-3%Si (under-stress measurements). The further increase of applied stress, implicitly of plastic strain, causes a progressive degradation of the magnetic behaviour. It is worthy of mention the clear difference between the magnetic properties measured under stress and after removal of the stress: Fe-3%Si and FeCo-2%V are magnetically degraded when the stress is removed, i.e. lower permeability and lower activity of domain walls (BN_{max}), while Ni is magnetically improved. The transition between the strain-hardening stages H.s.1 and H.s.2 of Fe-3%Si and Ni is clearly identified for both loaded and unloaded states.

4. Discussion

The effect of an applied elastic stress σ ($\sigma < \sigma_e$) on the magnetization of a ferromagnetic material is generally explained on the basis of the induced magnetoelastic energy E_σ, proportional to the tensorial product between the magnetostriction λ of the material and the applied stress [14]. According to Le Chatelier equilibrium principle, the domain structure is reorganised in order to minimise the magnetic free energy. The way in which the material respond to stress depends only on the sign of this product: the magnetisation in the stress direction is increased if the two terms, λ and σ, both have the same sign, and vice versa. The results presented in Fig. 2 are explained on the same basis. The magnetic degradation of Fe-3%Si and Ni under applied elastic stresses is a consequence of a corresponding negative macroscopic magnetostriction [14, 15]. The permeability decreases because of the formation of transverse magnetic domains. The number of 180° domain walls is reduced, leading to a decrease of the Barkhausen noise peak height [16]. As FeCo-2%V alloy has a positive magnetostriction (the saturation magnetostriction is close to 60×10^{-6}) [17], the opposite effect is observed: the permeability and the Barkhausen noise peak height increase.

The existence of two elastic strain stages could be due to the effect of the microyielding appearing before σ_e is reached, so E.s.1 would be a perfectly elastic strain stage and E.s.2 a microplastic yielding stage, as recently proposed by several authors [18, 19]. Indeed, geometrical-necessary dislocations are generated next to the grain boundaries to accommodate the strain between grains with different orientations. These dislocations act as pinning sites, reducing the mean free path of the domain walls displacement. This is clearly evidenced by the behaviour of FeCo-2%V alloy: the permeability and Barkhausen noise peak height start to decrease once the microyielding is initiated, for an applied stress of approximately 100 MPa.

In the plastic strain domain, the multiplication of dislocations leads to a slight but progressive deterioration of the magnetic behaviour. The permeability and the activity of domain walls are therefore reduced. This effect is more pronounced for the second strain-hardening stage H.s.2, because the walls of high density of dislocations are pinning sites of higher energy than the

isolated dislocations [20]. The difference between the under-stress states and the unloaded states in the plastic strain domain is the consequence of the effect of long-range internal stresses [10]. Indeed, after removal of the applied stress, the sample is characterized by a specific distribution of internal stresses: small tensile stress areas (mechanical hard regions) counterbalanced by wide compressive stress areas (mechanical soft regions). The hard regions are represented by the grain boundaries at the beginning of the plastic strain and by the tangles and walls of high density of dislocations for higher plastic strain rates [21]. The global magnetoelastic effect of this distribution is given by the compressive stress [14], which could be estimated by the kinematic hardening X. Ni, which keeps a negative magnetostriction, reaches therefore a favourable energetic state after removal of the stress (the magnetoelastic energy is negative for unloaded specimens). This leads to an augmentation of the permeability and of the domain walls activity. On the contrary, FeCo-2%V being characterized by a positive magnetostriction, the removal of the stress deteriorates its magnetic behaviour.

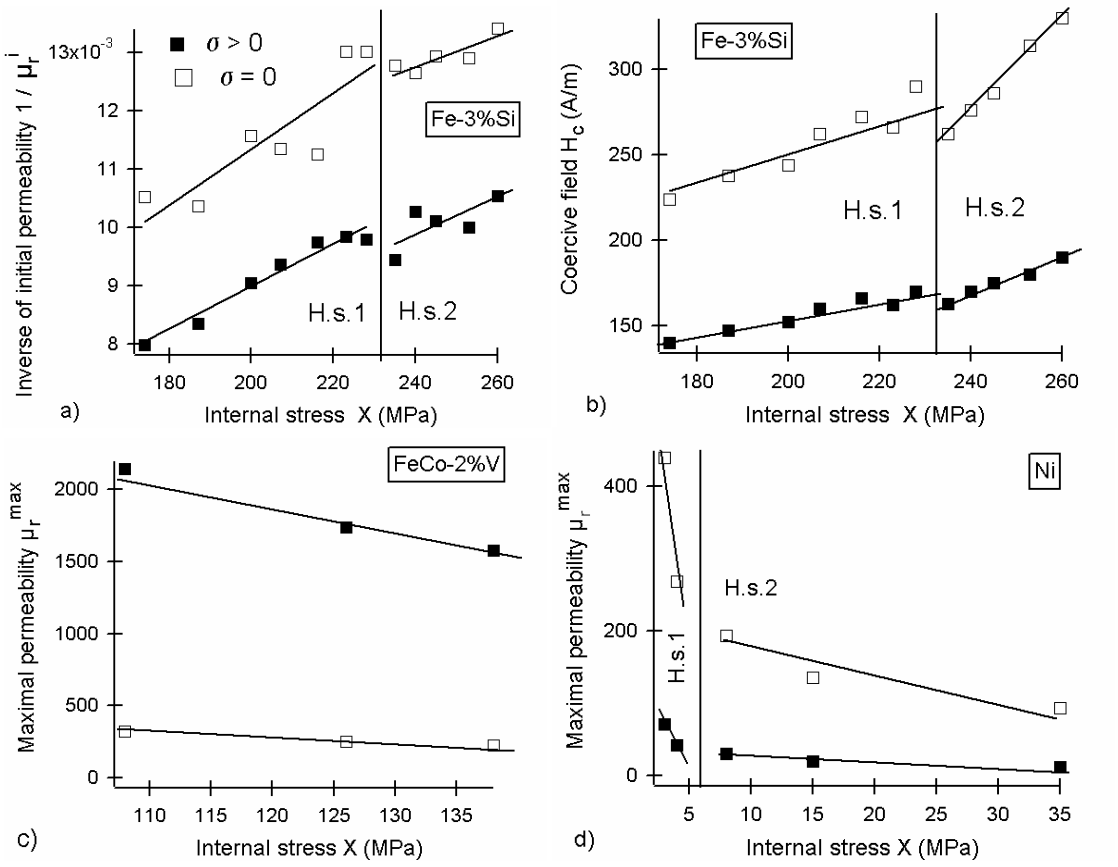

Fig. 3. Inverse of initial relative permeability $1/\mu_r^i$, maximal relative permeability μ_r^{max} and coercive field H_c versus internal stress X for under-stress states (full marks, $\sigma > 0$) and for the corresponding unloaded states (open marks, $\sigma = 0$) of the Fe-3%Si (a, b), FeCo-2%V (c) and Ni (d) specimens, in the plastic strain domain. Continuous lines represent linear regressions. The two hardening stages H.s.1 and H.s.2 for Fe-3%Si and for Ni are marked by delimitation lines.

As for Fe-3%Si, one could consider a possible similitude of its stress sensitivity to that of the polycrystalline iron, which presents a positive magnetostriction under compressive stresses [14]. The effect of a compressive stress being stronger than for the same amount of tensile stress, the electrical steel is magnetically deteriorated after removal of the stress.

The effect of internal stresses is also evidenced by the interesting results shown in Fig. 3. According to previous models proposed by Becker and Kondorski [15], the inverse of the initial permeability $1/\mu_r^i$ and the coercive field H_c have a linear relationship with the amount of internal stresses, which is the case of the results shown in Fig. 3a and Fig. 3b. Moreover, the same relationship is found for another parameters, like the maximal permeability μ_r^{max} (Fig. 3c, d). A close relationship between the evolution of the magnetic properties during strain-hardening and the kinematic hardening X is therefore confirmed.

5. Conclusions

This study reports an experimental characterization of a non-oriented Fe-3%Si steel lamination, a FeCo-2%V alloy and a high-purity polycrystalline nickel. Generally, the results attest the strong coupling between the magnetic properties and the deformation mechanisms of the materials. The pinning effect of dislocations are evidenced by the magnetic degradation during the microyielding stage and during strain-hardening. Interesting new results showing a clear difference between under-stress and unloaded states of plastically strained specimens and especially a linear relationship between magnetic properties and kinematic hardening X stand for the magnetoelastic effect of internal stresses. Further studies are in progress directed mainly to the development of predictive modelling of magnetomechanical interactions in electrical steel.

Acknowledgements

The financial cost of this work was supported by the Conseil Régional Picardie, France, pôle régional "multifonctionalité des matériaux et optimisation" (project no. 99.3). The authors thank Dr. F. Ossart from LMT-ENS Cachan France and Dr. N. Buiron from Roberval Laboratory – UTC France for useful discussions.

References

[1] O. Hubert, E. Hug, Mat. Sci. Tech. **11**, 482 (1995).
[2] A. Schoppa, J. Schneider, C. D. Wuppermann, J. Magn. Magn. Mater. **215-216**, 74 (2000).
[3] F. Ossart, Mec. Ind. **1**, 165 (2000).
[4] A. Kedous-Lebouc, B. Cornut, J. C. Perrier, Ph. Manfé, Th. Chevalier, J. Magn. Magn. Mater. **254-255**, 124 (2003).
[5] E. Hug, O. Hubert, M. Clavel, IEEE Trans. Mag. **33**, 763 (1997).
[6] O. Hubert, M. Clavel, I. Guillot, E. Hug, J. Phys. IV France **9**, 207 (1999).
[7] E. Hug, O Hubert, I. Guillot, J. Magn. Magn. Mater. **215-216**, 197 (2000).
[8] E. Hug, O. Hubert, J. J. Van Houtte, Mater. Sci. Engng. **A332**, 193 (2002).
[9] E. Hug, V. Iordache, RIGE **5**, 371 (2002).
[10] V. E. Iordache, E. Hug, N. Buiron, Mater. Sci. Engng. **A359**, 62 (2003).
[11] Y. Umakoshi, Mater. Sci. Tech. **6**, 251 (1993).
[12] V. E. Iordache, Doctorate Thesis, Université de Technologie de Compiègne, France, 2003.
[13] J. Lemaitre, J.-L. Chaboche, Mechanics of Solid Materials, Cambridge Univ. Press (1994).
[14] B. D. Cullity, Introduction to Magnetic Materials, Addison-Wesley Publishing Comp., New York (1972).
[15] R. M. Bozorth, Ferromagnetism, IEEE Press, New York (1993).
[16] T. W. Krause, L. Clapham, A. Pattantyus, D. L. Atherton, J. Appl. Phys. **79**, 4242 (1996).
[17] R. Boll, Mater. Sci. Tech. **3b**, 399 (1993).
[18] C. G. Stefanita, L. Clapham, D. L. Atherton, J. Mater. Sci. **35**, 2675 (2000).
[19] V. Moorthy, S. Vaidyanathan, T. Jayakumar, B. Raj, B. P. Kashyap, Acta Mater. **47**, 1869 (1999).
[20] J. Degauque, Solid State Phenomena **35-36**, 335 (1994).
[21] X. Feaugas, Acta Mater. **47**, 3617 (1999).